Article published online: 2021-01-29

Quantification of Early and Intermediate Age-related Macular Degeneration Using OCT "en face" Presentation

Quantifizierung der frühen und intermediären altersabhängigen Makuladegeneration mittels OCT-„en-face"-Darstellung

Authors
Frauke Jürgens[1], Kai Rothaus[1], Henrik Faatz[1], Britta Heimes-Bussmann[1], Daniel Pauleikhoff[1,2], Albrecht Peter Lommatzsch[1,2]

Affiliations
1 Retinologie, Augenzentrum am St. Franziskus-Hospital Münster, Deutschland
2 Zentrum für Augenheilkunde, Universität Duisburg-Essen, Duisburg, Deutschland

Key words
early and intermediate AMD, drusen area, number of drusen

Schlüsselwörter
frühe und intermediäre AMD, Drusenfläche, Drusenanzahl

received	21. 8. 2020
accepted	28. 10. 2020
published online	29.1.2021

Bibliography
Klin Monatsbl Augenheilkd 2022; 239: 79–85
DOI 10.1055/a-1327-3633
ISSN 0023-2165
© 2021. Thieme. All rights reserved.
Georg Thieme Verlag KG, Rüdigerstraße 14, 70469 Stuttgart, Germany

Correspondence
Frauke Jürgens
Retinologie, Augenzentrum am St. Franziskus-Hospital Münster
Hohenzollernring 74, 48145 Münster, Deutschland
Phone: + 49 (0) 25 19 35 27 11, Fax: + 49 (0) 25 19 35 27 19
frauke.juergens@gmx.de

ABSTRACT

Background Early and intermediate age-related macular degeneration (AMD) results in drusen deposits under the retinal pigment epithelium (RPE). These early stages of AMD exhibit different risks of progressing to late AMD. To date, early AMD has been classified and quantified by fundus photography. This does not appear to be sensitive enough for clinical trials studying the impact on drusen. SD-OCT with two-dimensional rendering of the segmented slices analysed allows for en face imaging of the drusen. The present trial studied the potential of quantifying early and intermediate AMD by en-face optical coherence tomography (OCT).

Material and Methods Thirty-one eyes of 29 patients in different stages of early and intermediate AMD were studied. To this end, fundus photographs (Kowa VX-10i, Kowa, Tokyo, Japan) and en-face OCT images (RTVue XR Avanti, Optovue, Inc., Fremont, CA, USA) were taken. First, different segmentation levels (6 µm underneath the RPE, on the RPE, 6 µm and 9 µm above the RPE) and different layer thicknesses (5 µm, 10 µm, 20 µm and 30 µm) were analysed to determine the best segmentation for visualising drusen. Drusen were marked manually and their number and surface area calculated. This analysis was then compared with the standardised drusen analyses on fundus photography. Additional changes in early and intermediate AMD such as pigment epithelial detachments (PEDs) and subretinal drusenoid deposits (SDD) as well as small atrophies were also documented and compared.

Outcomes The best segmentation for delineating the drusen on the en-face OCT images was found to be a segmentation 6 µm underneath the RPE with a slice thickness of 20 µm. Comparison of drusen quantification on en-face OCT images with the standardised drusen analysis on fundus photography revealed particularly good similarity. Other changes in early and intermediate AMD, such as PEDs, SDD and small atrophies, were easier to assess on the en-face OCT images.

Conclusions The analysis and quantification of drusen from en-face OCT images with 20 µm segmentation at 6 µm underneath the RPE allows differentiated quantification of various drusen characteristics. Moreover, other changes in early and intermediate AMD can also be analysed. In future observational and clinical trials, this could help quantify drusen.

ZUSAMMENFASSUNG

Hintergrund Bei der frühen und intermediären altersabhängigen Makuladegeneration (AMD) kommt es zu Ablagerungen unterhalb des retinalen Pigmentepithels (RPE) in Form von Drusen. Diese frühen Stadien der AMD beinhalten ein un-

This document was downloaded for personal use only. Unauthorized distribution is strictly prohibited.

terschiedliches Risiko zur Entwicklung einer späten AMD. Bisher erfolgte die Klassifizierung und Quantifizierung der frühen AMD anhand von Fundusfotos. Für klinische Studien, welche die Beeinflussung von Drusen überprüfen, erscheint dies zu wenig sensitiv. Das SD-OCT mit flächiger Darstellung segmentierter Analyseschichten ermöglicht eine En-face-Darstellung der Drusen. In der vorliegenden Studie wurden die Möglichkeiten einer Quantifizierung der frühen und intermediären AMD mit dem Verfahren des En-face-OCT untersucht.

Material und Methoden Es wurden 31 Augen von 29 Patienten mit früher und intermediärer AMD untersucht. Hierzu wurden Fundusfotos (Kowa VX-10i, Kowa, Tokyo, Japan) und En-face-OCT-Aufnahmen (RTVue XR Avanti, Optovue, Inc., Freemont, CA, USA) erstellt. Zunächst wurden verschiedene Schnittebenen (6 µm unterhalb des RPE, auf dem RPE, 6 µm und 9 µm oberhalb des RPE) und unterschiedlichen Schichtdicken (5, 10, 20 und 30 µm) analysiert, um die beste Segmentierung zur Darstellung der Drusen zu bestimmen. Die Drusen wurden manuell markiert und die Anzahl und Fläche berechnet. Diese Analyse wurde mit den standardisierten Drusenanalysen auf Fundusfotos verglichen. Zusätzliche Veränderungen einer frühen und intermediären AMD wie Pigmentepithelabhebungen (PEDs) und Subretinal drusenoid Deposits (SDD) sowie kleine Atrophien wurden ebenso dokumentiert und verglichen.

Ergebnisse Als beste Segmentierung zur Abgrenzung der Drusen auf den En-face-OCT-Aufnahmen konnte eine Segmentierung 6 µm unterhalb RPE mit einer Schnittdicke von 20 µm gefunden werden. Der Vergleich der Drusenquantifizierung auf En-face-OCT-Aufnahmen mit der standardisierten Drusenanalyse auf Fundusfotos zeigte eine sehr gute Vergleichbarkeit. Andere Veränderungen der frühen und intermediären AMD, wie PEDs, SDD und kleine Atrophien, waren auf den En-face-OCT-Aufnahmen besser beurteilbar.

Schlussfolgerung Die Analyse und Quantifizierung von Drusen auf En-face-OCT-Aufnahmen mit einer 20-µm-Segmentierung 6 µm unterhalb des RPE ermöglicht eine differenzierte Quantifizierbarkeit verschiedener Drusencharakteristika. Zudem können auch weitere Veränderungen der frühen und intermediären AMD analysiert werden. Dies könnte in zukünftigen Beobachtungs- und Behandlungsstudien zur Quantifizierung von Drusen eingesetzt werden.

Introduction

Age-related macular degeneration (AMD) is a degenerative disease of the retina near the macula and affects patients aged 50 and above [1]. To date, different classification systems are used worldwide, reflecting the clinical diversity of the disease [2].

In 2013, the AMD Classification Committee of the Beckmann Initiative for Macular Research developed a clinical classification system for AMD, which has been recognised and used internationally [3].

Early AMD is characterised by the presence of drusen (extracellular deposits underneath the pigment epithelium) and hyper- and/or hypopigmentation of the retinal pigment epithelium (RPE) [4]. Ferris et al. coined the term intermediate AMD to describe the advanced stage of early AMD. Here, the drusen diameter is more than 125 µm [3] (▶ **Fig. 1**).

Drusen are present in up to 80 % of the population over 60 years of age. They may be asymptomatic or induce metamorphopsia, especially with central soft drusen. Hard drusen are less than 63 µm in diameter and clinically recognisable as yellowish spots [5]. On ophthalmoscopy, soft drusen appear as yellowish-greyish, disc-shaped lesions and may be partly riddled with pigment changes. They may regress or coalesce. Confluent soft drusen induce a well-limited detachment of the RPE, the so-called drusenoid pigment epithelial detachment (DPED) [6, 7]. On ophthalmoscopy, subretinal drusenoid deposits (SDD) resemble the so-called regular drusen and are located temporally superior to the fovea. Their size ranges from 50 µm to 400 µm [8]. The clinical appearance of atrophy is a sharply defined, depigmented area. It may emerge de novo or develop from hyperpigmentation or drusen [9].

Today, the diagnostic workup of retinal disorders benefits from a broad range of digital examination modalities.

Colour fundus photography in particular is employed to document retinal changes and is of no primary diagnostic value. It plays an important role in many multicentre trials on AMD as well as other macular diseases [10].

The modality of choice in the study of macular changes is non-invasive optical coherence tomography [11]. It is a useful technique for visualising the drusen in early AMD.

This study aimed to explore the potential of a new quantification technique in early and intermediate AMD by en-face SD-OCT. Previously, classification and quantification of early and intermediate AMD (drusen) was based on fundus photography and assessment of drusen characteristics in the Early Treatment Diabetic Retinopathy (ETDRS) grid. This approach does not appear to be sensitive enough to determine the impact on drusen in clinical trials.

Materials and Methods

Patients with early or intermediate AMD were assessed in a consecutive case study. The inclusion criterion was the presence of soft drusen. The exclusion criterion was inadequate image quality in the pertinent imaging modalities.

The trial included 31 eyes of 29 patients with early or intermediate age-related macular degeneration and soft drusen. The mean patient age was 74.2 years. The youngest patient enrolled was 59 years old and the oldest patient 88 years. 22 patients were female and 7 male.

In 7 patients, the fellow eye also presented findings of early or intermediate AMD, in 23 patients there was exudative AMD and in one patient another disease. None of the patients had normal findings or geographic atrophy in the fellow eye.

This document was downloaded for personal use only. Unauthorized distribution is strictly prohibited.

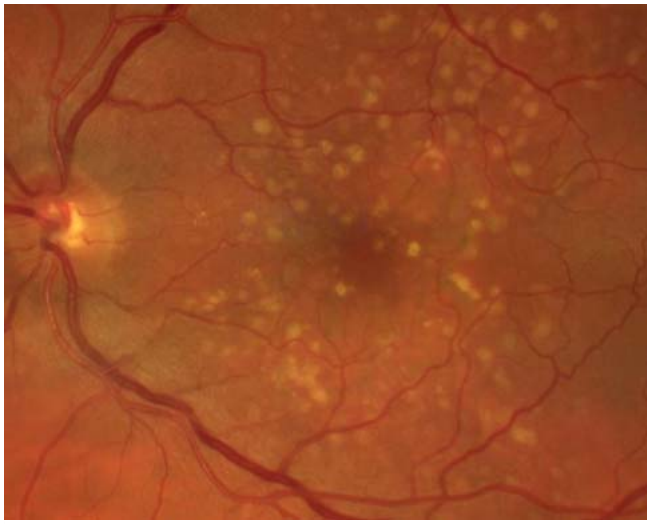

▶ **Fig. 1** Fundus photograph of intermediate AMD with soft drusen, hard drusen, hypo- and hyperpigmentation.

The RTVue XR Avanti OCT unit (Optovue, Inc., Fremont, CA, USA) with the AngioVue software package allows en-face imaging of the retina in defined slices (segmentations).

To best assess the extent of the soft drusen, a suitable slice had to be defined first. To this end, 20 patients with soft drusen in early or intermediate AMD were imaged with Avanti OCT. En-face images were obtained in different slices with respect to the RPE (6 µm underneath the RPE, on top of the RPE, 6 µm above the RPE, and 9 µm above the RPE) and in different slice thicknesses (5 µm, 10 µm, 20 µm, and 30 µm) and the images were then compared (▶ **Fig. 2**).

Slice analysis was performed with 3 × 3 mm^2 images. The acceptable tolerance was ± 1 µm. Soft drusen were visible in the images as dark (hyporeflective) areas. Subjectively, the greater the slice thickness, the fuzzier the drusen appeared. The smaller the distance to the RPE, the more clearly delimited the drusen area appeared. The further above the RPE, the smaller the drusen areas appeared and the more common the artefacts. Artefacts were defined as hyporeflective areas on en-face imaging, but which could not be confirmed as drusen in the horizontal slice Artefact formation was particularly evident in shallow, confluent drusen and in remarkably close, steeply rising drusen.

In the plane just underneath the RPE from 6 µm to 25 µm, good delineation of the extent of the drusen was seen in all patients, so that this slice was taken as the standard for further examination.

Thirty-one eyes in 29 patients were examined by Avanti OCT. The en-face images of the 3 × 3 mm2 retinal sections were visualised as described previously and saved as. jpg files. The parameters were analysed with the ImageJ 1.50i software (National Institutes of Health, Bethesda, MD, USA). First, the size of the image section with the corresponding image pixels was defined as 3 × 3 mm^2 in each case. Soft drusen were shown as black areas. The AngioVue software of the Avanti OCT checked each black area in parallel to determine whether it was a druse or artefact (▶ **Fig. 3**).

The ImageJ software marked each drusen area in black. The marked areas were highlighted against the remaining image background with the Threshold Colour function. The number and sur-

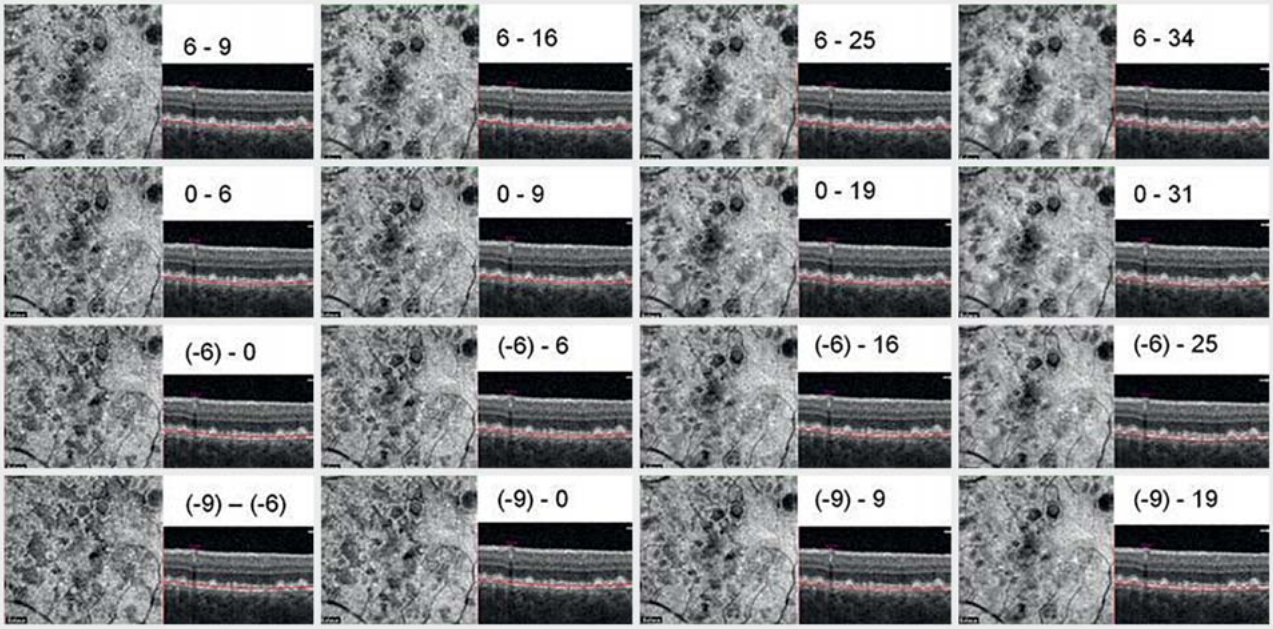

▶ **Fig. 2** Example of en-face drusen imaging by Avanti OCT with different slice thicknesses and distances from the RPE. Values in µm relative to the RPE. Positive values refer to areas underneath the RPE, negative values to those above the RPE.

This document was downloaded for personal use only. Unauthorized distribution is strictly prohibited.

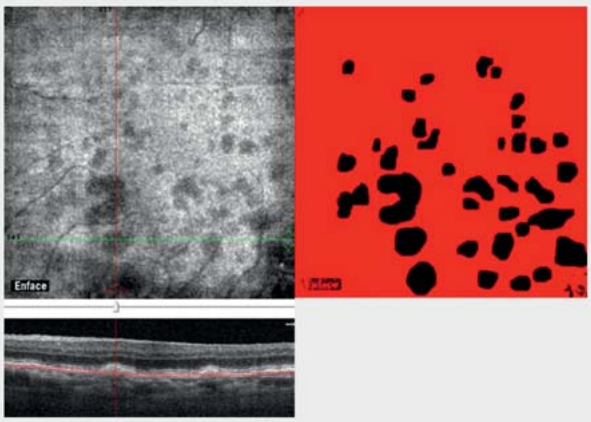

▶ **Fig. 3** Example of drusen analysis in en-face imaging in the slice 6 µm to 25 µm underneath the RPE: Checking the black area in en-face imaging in the corresponding B-scan, paralleled by marking of the drusen area in the ImageJ software.

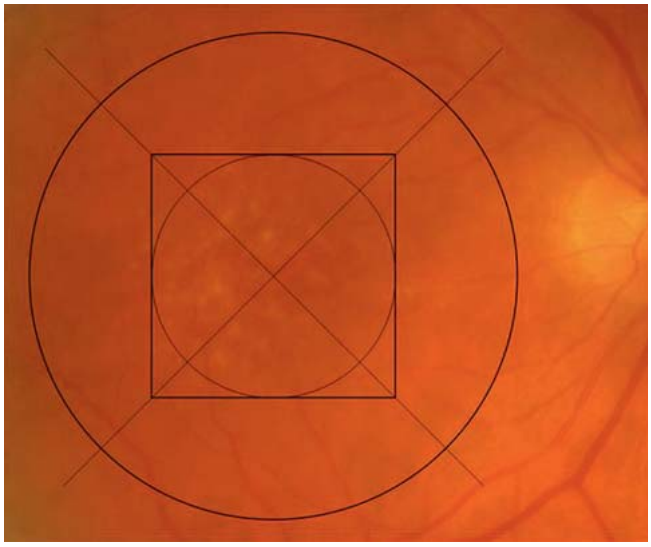

▶ **Fig. 4** Fundus photography with corresponding overlay of the square grid with the EDTRS grid.

face area of the drusen were assessed based on this image. The surface area was calculated with the help of the "ROI Manager" (ROI: Region of Interest) function.

B-scans of the corresponding area were assessed to see whether the examined eye displayed atrophy, PED or SDD.

Digital fundus images were taken with the Kowa fundus camera VX-10i (Kowa, Tokyo, Japan) and visualised and assessed with the software Heidelberg Eye Explorer v. 1.0.10.0 and above or with the software HEYEX Viewer version 6.5.7.0.

Fundus photography assessment was based on the international classification of Bird et al [1] but was heavily modified for better comparability with OCT images. For example, a square grid was created and the central 3 × 3 mm^2 area was assessed. Due to the different scales of the fundus images, the square grid was combined with the ETDRS grid (ETDRS: Early Treatment Diabetic Retinopathy Study), printed on film and adjusted on the monitor to the corresponding scale of the fundus image. With the ETDRS grid on Spectralis OCT, three intersections each with the retinal vessels were located and superimposed on the screen (▶ **Fig. 4**).

Measurement of the drusen area was also based on the international classification. In each of the central four sections (superior, nasal, inferior, and temporal), the percentage of drusen area was estimated and converted to the corresponding area in mm^2.

The largest druse was measured and converted to scale.

The assessment of any presence of atrophy, PED or reticular pseudodrusen was carried out by looking at the fundus image.

Outcomes

In both measurement techniques, the number of soft drusen correlated with the drusen area. The more soft drusen were present, the larger was their area (Spearman rank correlation rho = 0.731; $p = 0.001 < 0.05$ (OCT Avanti) and rho = 0.581; $p = 0.0006 < 0.05$ (fundus photography)).

The mean area of soft drusen as measured by Avanti OCT was 1.86 mm^2, and 1.75 mm^2 with fundus photography. There was no statistically significant difference between the Avanti OCT and fundus photography measurements (Wilcoxon test for paired samples: $n = 31$; $p = 0.4331 > 0.05$) (▶ **Fig. 5**).

Passing-Bablok regression revealed no statistically significant systematic differences between the two modalities (rank correlation according to Spearman rho = 0.697; $p < 0.0001 < 0.05$). The equation for the slope of the regression line is: $y = -0.106 + 1.132\,x$ (▶ **Fig. 6**).

There was a major difference in PED identification by Avanti OCT and fundus photography imaging modalities. Avanti OCT detected a total of 16 PEDs, whereas fundus photography identified only 8 PEDs.

The differences in atrophy detection were smaller. Avanti OCT identified atrophy in 6 eyes, while fundus photography detected atrophy in 5 eyes.

In the en-face image, Avanti OCT could not visualize subretinal drusenoid deposits in the retinal slice examined. Assessment was based on the B-scans. Avanti OCT revealed SDD in 7 eyes, while fundus photography identified SDD in 6 eyes.

All changes seen on fundus photography were also picked up by Avanti OCT. ▶ **Table 1** presents an overview.

Data analysis was performed with the MedCalc Statistical Software version 17.9.7 (MedCalc Software bvba, Oostend, Belgium).

The analysis of some morphological parameters was descriptive, as the sample size was too small for statistical testing for correlations and differences.

The rank correlation coefficient according to Spearman was determined to determine if there was a monotonic correlation between two variables. Pearson's coefficient of correlation and Passing-Bablock regression were used to compare two measurement methodologies. Wilcoxon's test for paired samples was used to test the equivalence of the central tendencies of two samples.

This document was downloaded for personal use only. Unauthorized distribution is strictly prohibited.

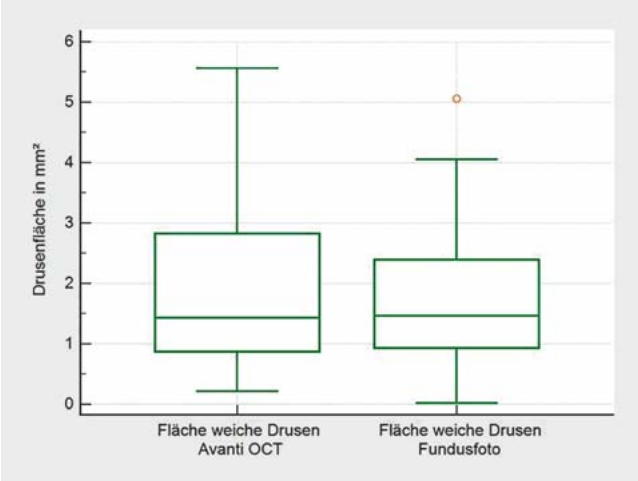

▶ **Fig. 5** Comparison of the soft drusen area as measured by Avanti OCT and fundus photography.

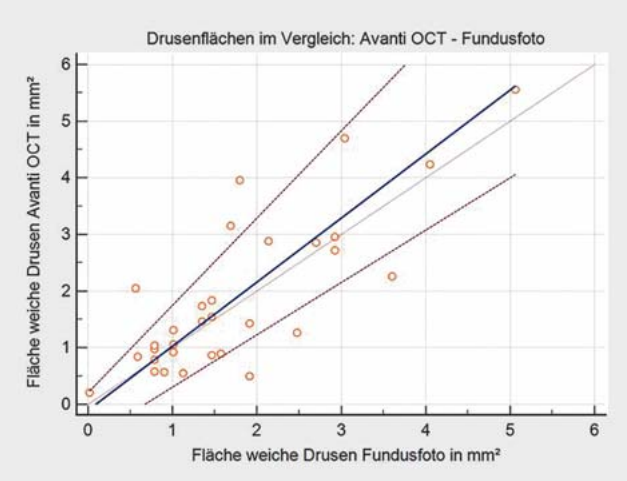

▶ **Fig. 6** Distribution diagram of the drusen areas as measured by Avanti OCT and fundus photography.

Discussion

Numerous studies have been published on the manual and/or automated quantification of drusen in fundus photography and OCT [12–17]. This shows the effort to develop an alternative and replicable approach to quantifying drusen material. In current clinical trials on AMD, analysis and staging is based on fundus photography. Assessment is performed manually by well-trained so-called "graders" who evaluate the fundus photographs according to the given parameters in each case.

Fundus photography assessment has already seen several attempts at computer-assisted drusen measurement. Most often, the aim was to develop an automated approach to determine the number, area, and size of the drusen and to measure progression (in terms of a change in drusen area) over time [18, 19].

The previous method of assessing drusen by fundus photography was used to evaluate the new method of visualising drusen areas on OCT. In addition to the drusen surface area measurement, further parameters important for the assessment of early AMD were collected for both examination techniques.

PED analysis revealed quite different outcomes. The markedly higher number of PEDs on Avanti OCT may have been due to better assessment of the drusen areas in relation to the detached RPE. In fundus photography, a possibly blurred delineation to the "healthy" retina may have resulted in the druse measurements being smaller than they were. The difference between both examination techniques in atrophy identification was only minor. However, it should be noted that the number of atrophies was neglected, and the size of the atrophies was not compared. SDD assessment also revealed a rather small difference between both imaging modalities, although the analysis was quite different. The SDDs were detected on the fundus photography in a markedly temporal location superior to the fovea. SDD assessment by Avanti OCT was only possible on B-scan, and here no preferred location was seen.

▶ **Table 1** PED, atrophy and SDD as measured by Avanti OCT and fundus photography.

	Avanti		Image	
	SDD	**%**	**SDD**	**%**
Yes	7	22.58	6	19.35
No	24	77.42	25	80.65
Overall	31	100.00	31	100.00
	Atrophy	**%**	**Atrophy**	**%**
Yes	6	19.35	5	16.13
No	25	80.65	26	83.87
Overall	31	100.00	31	100.00
	PED	**%**	**PED**	**%**
Yes	16	51.61	8	25.81
No	15	48.39	23	74.19
Overall	31	100.00	31	100.00

Both fundus photography and OCT Avanti demonstrated a positive correlation between the number of soft drusen and the area of soft drusen. Particularly in advanced stages and large drusen, the drusen can also coalesce, which in turn would reduce the number of drusen. A trial by Diniz et al compared manual drusen area measurement on colour fundus photography, retromode scanning laser ophthalmoscopy and automated area measurement on Cirrus HD-OCT (Carl Zeiss, Meditec, Inc). Automated measurements yielded a significantly smaller number of drusen than the images analysed by hand. However, area measurement was comparable, suggesting that the algorithm counts confluent drusen as a single druse [15].

In this trial, the area measurement in both modalities was comparable, while the additional parameters collected on early AMD were assessed more accurately on SD-OCT. When combined with

This document was downloaded for personal use only. Unauthorized distribution is strictly prohibited.

cross-sectional assessment (B-scan), the visualisation of the drusen area allows for a better and more accurate analysis of these areas, PEDs, atrophies, and reticular drusen, but also requires significantly more time. Automated area measurement without neglecting small and shallow drusen would be desirable, as has already been described in the literature [15–17].

Gregori et al. assessed the drusen areas measured on fundus photography as well as SD-OCT using Cirrus HD-OCT regarding the progression of the drusen areas. In this study, the drusen areas measured on SD-OCT were smaller than on digital fundus photography because the automated measurement neglects small, shallow and subretinal drusenoid deposits. The authors believe that automated drusen area measurement is nevertheless important in everyday clinical practice, as medium-sized and large drusen in particular play a significant role in the progression of early AMD. They also point out that an automated, standardised measurement is more comparable over time [16].

Unlike the results of Gregori et al., the drusen areas measured in this trial were larger on SD-OCT than on fundus photography. It must be noted here that the manual measurements included any shallow and small RPE elevation resulting from drusenoid deposits. While for everyday clinical practice, automated measurement of the drusen area is much more practical, it is important to understand the limits of automated measurements.

Artificial intelligence (AI) through deep learning and/or machine learning opens further avenues for automated image analysis in AMD [20–23]. These are "intelligent" decision-making processes performed by machines. While machine learning uses algorithms to learn skills, deep learning employs a deep neural network to analyse data [24].

It has also been shown that the new AI techniques can be used effectively in AMD detection, staging and prediction [25]. In a study by Burlina et al., fundus photography, following the staging of the ARED study, deep learning, and physician assessment yielded comparable results in AMD staging [26]. Lee et al. studied the feasibility of analysing OCT images using deep learning to differentiate between a healthy retina and existing AMD [20]. Venhuizen et al. were also able to demonstrate that AMD staging based on OCT images by machine learning and physician assessment yielded similar results. The benefit of machine learning is seen in the fast and reliable analysis of large numbers of OCT images, especially in large AMD trials. It also offers the potential for OCT-based AMD screening [22].

Conclusions

Despite some limitations, especially due to the small patient sample, this trial was able to develop a technique for quantifying drusen in early and intermediate AMD, which can be applied to different examination tools. The condition here is the ability to perform en-face imaging in a defined retinal slice. Although some studies prefer to analyse drusen volumes to quantify AMD [13, 14], drusen area plays a major role.

The technique described here also allows the assessment of other retinal changes in early and intermediate AMD, such as atrophy, PED and SDD. It is comparable to the previous approach of fundus photography assessment and is even more sensitive in some respects, such as drusen delineation.

However, due to the time required, this method of quantifying and classifying early and intermediate AMD is not feasible for everyday clinical practice and trials, and in a next step the potential of an automated procedure needs to be studied.

The inclusion of artificial intelligence (AI) in terms of machine learning and deep learning may also offer great benefits here.

Conflict of Interest

The authors declare that they have no conflict of interest.

References

[1] Bird AC, Bressler NM, Bressler SB et al. An international classification and grading system for age-related maculopathy and age-related macular degeneration. Surv Ophthalmol 1995; 39: 367–374. doi:10.1016/s0039-6257(05)80092-x

[2] Deutsche Ophthalmologische Gesellschaft. Nahrungsergänzungsmittel bei altersabhängiger Makuladegeneration. Aktuelle Stellungnahme der Deutschen Ophthalmologischen Gesellschaft, der Retinologischen Gesellschaft und des Berufsverbandes der Augenärzte Deutschlands (Stand Oktober 2014). Klin Monbl Augenheilkd 2015; 232: 196–201. doi:10.1055/s-0034-1396155

[3] Ferris FL, Wilkinson CP, Bird A et al. Clinical classification of age-related macular degeneration. Ophthalmology 2013; 120: 844–851. doi:10.1016/j.ophtha.2012.10.036

[4] Lim LS, Mitchell P, Seddon JM et al. Age-related macular degeneration. Lancet 2012; 379: 1728–1738. doi:10.1016/S0140-6736(12)60282-7

[5] von Strachwitz CN. Trockene altersabhängige Makuladegeneration. Ophthalmologe 2013; 110: 555–565. doi:10.1007/s00347-012-2757-y

[6] Hartnett ME, Weiter JJ, Garsd A et al. Classification of retinal pigment epithelial detachments associated with drusen. Graefes Arch Clin Exp Ophthalmol 1992; 230: 11–19. doi:10.1007/bf00166756

[7] Cukras C, Agrón E, Klein ML et al. Natural history of drusenoid pigment epithelial detachment in age-related macular degeneration: age-related eye disease study report no. 28. Ophthalmology 2010; 117: 489–499. doi:10.1016/j.ophtha.2009.12.002

[8] Schmitz-Valckenberg S, Steinberg JS, Fleckenstein M et al. Combined confocal scanning laser ophthalmoscopy and spectral-domain optical coherence tomography imaging of reticular drusen associated with age-related macular degeneration. Ophthalmology 2010; 117: 1169–1176. doi:10.1016/j.ophtha.2009.10.044

[9] Fleckenstein M, Schmitz-Valckenberg S, Sunness JS et al. Geographische Atrophie. In: Holz FG, Pauleikhoff D, Spaide RF, Bird AC, Hrsg. Altersabhängige Makuladegeneration. Berlin, Heidelberg: Springer; 2011: 125–141. doi:10.1007/978-3-642-20870-6_8

[10] Heimann H, Kellner U. Fundusfotografie und Weitwinkelsysteme. In: Heimann H, Kellner U, Hrsg. Atlas des Augenhintergrundes. Stuttgart: Thieme; 2010. doi:10.1055/b-0034-40446

[11] Kellner S, Rüther K. Prinzipien der Diagnostik retinaler Erkrankungen. Augenheilkunde up2date 2013; 3: 219–237. doi:10.1055/s-0032-1325094

[12] Nathoo NA, Or C, Young M et al. Optical coherence tomography-based measurement of drusen load predicts development of advanced age-related macular degeneration. Am J Ophthalmol 2014; 158: 757–761.e1. doi:10.1016/j.ajo.2014.06.021

[13] Nittala MG, Ruiz-Garcia H, Sadda SR. Accuracy and reproducibility of automated drusen segmentation in eyes with non-neovascular age-related macular degeneration. Invest Ophthalmol Vis Sci 2012; 53: 8319–8324

This document was downloaded for personal use only. Unauthorized distribution is strictly prohibited.

[14] Freeman SR, Kozak I, Cheng L et al. Optical coherence tomography-raster scanning and manual segmentation in determining drusen volume in age-related macular degeneration. Retina 2010; 30: 431–435. doi:10.1097/IAE.0b013e3181bd2f94

[15] Diniz B, Ribeiro R, Heussen FM et al. Drusen measurements comparison by fundus photograph manual delineation versus optical coherence tomography retinal pigment epithelial segmentation automated analysis. Retina 2014; 34: 55–62. doi:10.1097/IAE.0b013e31829d0015

[16] Gregori G, Yehoshua Z, Garcia Filho CA et al. Change in drusen area over time compared using spectral-domain optical coherence tomography and color fundus imaging change in drusen area over time: SDOCT Versus CFIs. Invest Ophthalmol Vis Sci 2014; 55: 7662–7668

[17] Yehoshua Z, Gregori G, Sadda SR et al. Comparison of drusen area detected by spectral domain optical coherence tomography and color fundus imaging. Invest Ophthalmol Vis Sci 2013; 54: 2429–2434

[18] Kumari K, Mittal D. Drusen quantification for early identification of age related macular degeneration. Adv Image Video Process 2015; 3: 28–40. doi:10.14738/aivp.33.1291

[19] van Grinsven MJ, Lechanteur YT, van de Ven JP et al. Automatic drusen quantification and risk assessment of age-related macular degeneration on color fundus images. Invest Ophthalmol Vis Sci 2013; 54: 3019–3027

[20] Lee CS, Baughman DM, Lee AY. Deep learning is effective for the classification of OCT images normal versus Age-related Macular Degeneration. Ophthalmol Retina 2017; 1: 322–327. doi:10.1016/j.oret.2016.12.009

[21] Fang L, Cunefare D, Wang C et al. Automatic segmentation of nine retinal layer boundaries in OCT images of non-exudative AMD patients using deep learning and graph search. Biomed Opt Express 2017; 8: 2732–2744. doi:10.1364/boe.8.002732

[22] Venhuizen FG, van Ginneken B, van Asten F et al. Automated Staging of Age-Related Macular Degeneration Using Optical Coherence Tomography. Invest Ophthalmol Vis Sci 2017; 58: 2318–2328. doi:10.1167/iovs.16-20541

[23] Schmidt-Erfurth U, Waldstein SM, Klimscha S et al. Prediction of Individual Disease Conversion in Early AMD Using Artificial Intelligence. Invest Ophthalmol Vis Sci 2018; 59: 3199–3208. doi:10.1167/iovs.18-24106

[24] Treder M, Eter N. Chancen von künstlicher Intelligenz und Big Data für die Diagnostik und Behandlung der altersabhängigen Makuladegeneration. Klin Monbl Augenheilkd 2019; 236: 1418–1422. doi:10.1055/a-1012-2036

[25] Schmidt-Erfurth U, Sadeghipour A, Gerendas BS et al. Artificial intelligence in retina. Prog Retin Eye Res 2018; 67: 1–29. doi:10.1016/j.preteyeres.2018.07.004

[26] Burlina P, Pacheco KD, Joshi N et al. Comparing humans and deep learning performance for grading AMD: A study in using universal deep features and transfer learning for automated AMD analysis. Comput Biol Med 2017; 82: 80–86. doi:10.1016/j.compbiomed.2017.01.018

This document was downloaded for personal use only. Unauthorized distribution is strictly prohibited.